Heliyon 10 (2024) e30505

Contents lists available at ScienceDirect

Heliyon

journal homepage: www.cell.com/heliyon

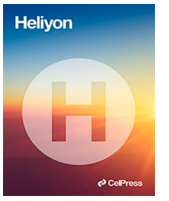

Research article

The role of *FERMT2* in the tumor microenvironment and immunotherapy in pan-cancer using comprehensive single-cell and bulk sequencing

Guang-hao Wu [a,1], Chao He [b,1], Gang Che [b,1], Zheng Zhou [b], Bi-ying Chen [b], Hai-ming Wu [c], Jian-feng Chen [c], Wei-pu Zhu [d], Yan Yang [b], Zhan Zhou [e,**], Li-song Teng [b,***], Hai-yong Wang [b,*]

[a] *School of Clinical Medicine, Hangzhou Normal University Medical College, Hangzhou, China*
[b] *Department of Surgical Oncology, The First Affiliated Hospital, School of Medicine, Zhejiang University, Hangzhou, China*
[c] *Department of Gastrointestinal Surgery, Yiwu Central Hospital, Jinhua, China*
[d] *MOE Key Laboratory of Macromolecular Synthesis and Functionalization, Department of Polymer Science and Engineering, Zhejiang University, Hangzhou, China*
[e] *Institute of Drug Metabolism and Pharmaceutical Analysis and Zhejiang Provincial Key Laboratory of Anti-Cancer Drug Research, College of Pharmaceutical Sciences, Zhejiang University, Hangzhou, China*

ARTICLE INFO

Keywords:
Pan-cancer
Tumor microenvironment
Single-cell transcriptomics
Cancer-associated fibroblasts

ABSTRACT

FERMT2 has been identified as a participant in integrin-linked kinase signaling pathways, influencing epithelial-mesenchymal transition and thereby affecting tumor initiation, progression, and invasion. While the character of *FERMT2* in the tumor microenvironment (TME) as well as its implications for immunotherapy remain unclear. Thus, we conducted a comprehensive analysis to assess the prognostic significance of *FERMT2* using Kaplan-Meier analysis. In addition, we employed enrichment analysis to uncover potential underlying molecular mechanisms. Using "Immunedeconv" package, we evaluated the immune characteristics of *FERMT2* within TME. Furthermore, we determined the expression levels of *FERMT2* in various cell types within TME, based on single-cell sequencing data. To confirm the co-expression of *FERMT2* and markers of cancer-associated fibroblasts (CAFs), we performed multiplex immunofluorescence staining on tissue paraffin sections across various cancer types. Our analysis disclosed a significant correlation between elevated *FERMT2* expression and unfavorable prognosis in specific cancer types. Furthermore, we identified a strong correlation between *FERMT2* expression and diverse immune-related factors, including immune checkpoint molecules, immune cell infiltration, microsatellite instability (MSI), and tumor mutational burden (TMB). Additionally, there was a significant correlation between FERMT2 expression and immune-related pathways, particularly those associated with activating, migrating, and promoting the growth of fibroblasts in diverse cancer types. Interestingly, we observed consistent co-expression of *FERMT2* in both malignant tumor cells and stromal cells, particularly within CAFs. Notably, our findings also indicated that

* Corresponding author. Department of Surgical Oncology, The First Affiliated Hospital, School of Medicine, Zhejiang University; No.79 Qingchun Road, Shangcheng District, Hangzhou, Zhejiang Province, China.
** Corresponding author.
*** Corresponding author.
E-mail addresses: zhanzhou@zju.edu.cn (Z. Zhou), lsteng@zju.edu.cn (L.-s. Teng), lanceter1@zju.edu.cn (H.-y. Wang).
[1] These authors contribute equally to this work.

https://doi.org/10.1016/j.heliyon.2024.e30505
Received 7 December 2023; Received in revised form 29 April 2024; Accepted 29 April 2024
Available online 1 May 2024

FERMT2, in particular, exhibited elevated expression levels within tumor tissues and co-expressed with *α-SMA* in CAFs based on the multiplex immunofluorescence staining results.

1. Introduction

Cancer poses a significant obstacle to achieving higher life expectancy worldwide. By the end of the century, it is anticipated that cancer will become the leading cause of premature death in many countries, surpassing cardiovascular diseases [1]. In recent years, the global incidence of cancer has shown a consistent upward trend [2,3]. According to research conducted by the International Agency for Research on Cancer, it is projected that the global incidence of cancer will reach 28.4 million cases by 2040, reflecting a 47 % rise compared to 2020 [4].

Recently, there has been increasing interest in research on the TME. Studies suggest that cancer progression is a dynamic and continuous process, wherein cancer cells primarily interact with components within the TME to support local invasion and metastasis [5]. Within the TME of various cancer types, there are various types of non-cancerous cells, encompassing endothelial cells, normal and cancer-associated fibroblasts, immune cells, along with non-cellular elements including cytokines, chemokines, as well as growth factors [6].

Given the significant importance of the TME in cancer biology, cancer research and treatment have shifted their focus from a tumor-centric to a TME-centric pattern due to the significant importance of the TME in cancer biology [7]. In addition to traditional approaches such as surgical resection, chemotherapy, and radiation therapy targeting the primary tumor, immune checkpoint inhibitors (ICIs) directed towards specific immune cells have become a pivotal immunotherapeutic strategies in clinical practice [8].

Immune checkpoints play a role in maintaining immune tolerance within the body, but cancer cells often exploit this mechanism to disguise themselves as normal cells, thereby evading immune surveillance [9]. *CTLA-4* weakens the activation of memory T cells as well as naïve T cells by binding to its corresponding ligand, while the function of T cells in adjacent tissue area are primarily modulated by PD-1 via the interaction with its receptor *PD-L1* [8,10]. An increasing body of evidence confirms the remarkable ability of ICI therapy to significantly prolong the survival of cancer patients, underscoring its immense clinical utility. This approach holds great promise in revolutionizing cancer treatment by leveraging the intricate interactions within the TME to boost the body's innate immune response [11–13]. Despite the impressive advancements achieved with ICI therapy, limitations such as a restricted response rate and unpredictable efficacy persist. So we need to uncover a reliable predictive biomarker to determine individual variations in immunotherapy sensitivity, thereby enhancing personalized treatment for patients [8,14].

FERMT2 belongs to the family of focal adhesion protein, and is involved in numerous physiological processes in the human body. The absence of *FERMT2* often leads to alterations in the composition of cortical actin, thereby affecting skeletal muscle development [15]. In recent years, research on *FERMT2* has revealed potential correlations with certain cancers. The expression of *FERMT2* has been found to be associated with various tumors, such as pancreatic cancer, and breast cancer. In these cancers, *FERMT2* participates in integrin-linked kinase signaling pathways to regulate integrin activation, thereby influencing tumor initiation and progression [16–18]. Additionally, studies have indicated that the elevated level of *FERMT2* can promote local progression and metastasis of tumor in oral cancer as well as gallbladder cancer by modulating epithelial-mesenchymal transition (EMT) [19,20]. Furthermore, in colorectal cancer, *FERMT2* can affect EMT of cancer cells through the activation of Wnt/β-catenin signaling pathway, thus influencing tumor advancement [21].

However, the exact character of *FERMT2* in TME and its specific mechanisms in different types of tumors remain insufficiently elucidated. Therefore, we conducted a comprehensive investigation of the role of *FERMT2 in the* pan-cancer context. Apart from discovering the relations between expression levels of *FERMT2* and prognostic outcomes in pan-cancer context, moreover, we explored the associations between *FERMT2 expression pattern* and immune cell infiltrations, immunotherapy response, as well as potential molecular mechanisms. Furthermore, we validated our previous conclusions using large scale single-cell sequencing data and immunohistochemical staining techniques.

2. Materials and methods

2.1. Acquisition of data and sample collection

We acquired comprehensive RNA sequencing data, somatic mutation profile and corresponding clinical attributes of 33 tumor types, along with their respective normal counterparts, from TCGA database. In addition, RNA sequencing data from 31 kinds of normal tissues were retrieved from the GTEx database. Gene expression profiles of cell lines were sourced from the CCLE database, while gene expression data across various tissues were acquired from the HPA database. We retrieved single-cell sequencing data of various cancer types, including breast carcinoma (BRCA, GSE118389), kidney renal clear cell carcinoma (KIRC, GSE171306), bladder cancer (BLCA, GSE145137), head and neck squamous cell carcinoma (HNSC, GSE103322), stomach adenocarcinoma (STAD, GSE183904), liver hepatocellular carcinoma (LIHC, GSE125449), and prostate adenocarcinoma (PRAD, GSE137829). We also acquired single cell sequencing data from distinct subtypes of CAFs, along with normal fibroblasts (NFs), from the dataset GSE210347. All human paraffin sections of primary tumor as well as adjacent normal tissues were obtained from The First Affiliated Hospital of Zhejiang University, Hangzhou, China. After signing the informed consent, tissue samples of local tumor and peripheral normal areas were collected in accordance with ethical guidelines and regulations.

2.2Prognostic significance of FERMT2

FERMT2 expression patterns were extracted from each tumor sample according to TCGA database along with the matching clinical features. Two primary outcome measures, overall survival (OS) as well as disease-specific survival (DSS), are employed to investigate the prognostic impact of *FERMT2* expression patterns. We used the "survival" R package to conduct univariate Cox analysis, while the "forestplot" R package was utilized for generating forest plots as well as Kaplan-Meier survival curves.

2.3. Underling potential molecular mechanisms

The immune-related gene sets were obtained from GO terms, and the "GSVA" R package was applied to conduct GSVA. Meanwhile, GSEA was executed using the "GSEA" command within the "clusterProfiler" R package. The annotated datasets encompassed both the KEGG gene set and the Hallmark gene set.

2.4. Evaluation of tumor microenvironment

The "ESTIMATE" R package was employed to quantify stromal score and immune gene set enrichments score within each tumor sample. The resulting individual scores were then aggregated to derive a cumulative ESTIMATE score, which serves as a conclusive assessment of tumor purity. Subsequently, within certain cancer types, the correlation between *FERMT2* expression patterns and the aforementioned scores was visualized via applying the "ggplot 2″ R package. Moreover, the "Immunedeconv" R package [22] was utilized to uncover the association between *FERMT2* expression patterns and immune cell infiltration in pan-cancer context. The outcomes were then presented through correlation heatmaps.

2.5. Data processing of single-cell sequencing

The copycat R package utilizes integrative Bayesian techniques to infer genomic copy numbers and subclonal structures, enabling the identification of genome-wide aneuploidy within single cells. In this study, copycat was employed to discern aneuploid (tumor) cells from diploid (normal) cells based on high-throughput sc-RNAseq data. Subsequent steps involved filtering out poor-quality cells and genes based on the following criteria: (a) unique molecular identifiers (UMI) of cells were fewer than 400; (b) expression of mitochondria-related genes of cells beyond 20 %; (c) genes detected in less than three cells.

To address undesirable variations, normalization and scaling procedures were implemented in accordance with established protocols. Gene expression matrix of each remaining cells was subject to normalization utilizing a global-scaling approach, employing a default scaling number of 10,000. Subsequently, a natural-log transformation (log (1 + x)) was applied to the data, facilitated by the utilization of the "NormalizeData" command within the Seurat software. The process of identifying genes with variable expression involved employing the "FindVariableGenes" function utilizing the "vst" selection method, encompassing a feature count of 2000. Subsequently, to lower dimensionality, this set of 2000 genes exhibiting variability underwent principal component analysis.

Utilizing the "FindClusters" function, cluster analysis was conducted as per a default resolution parameter of 0.5. The ensuing Louvain clusters were visually depicted within a two-dimensional UMAP representation, and their identification with recognized cell types was manually accomplished via the utilization of canonical marker genes. Visual presentations of the data encompassing Vlnplot, Dimplot, and Featureplot were generated following the relevant commands provided in the Seurat manual.

2.6. Immunoblot analysis

The total proteins of cultured cells were extracted using RIPA buffer (Beyotime Inc., China) supplemented with 1 % phosphatase and protease inhibitors. After centrifugation of cell lysates at 1.2 × 10^4 g, 4 °C for 30 min, the supernatant was collected. The protein concentrations were measured using the BCA Protein assay kit (Thermo Scientific, USA). Equal amounts of protein (30 μg) were loaded onto each lane, separated by SDS-PAGE, which was transferred to PVDF membranes afterwards (Millipore, USA). The membranes, after blocked for 15mins, were incubated with primary antibodies (shown below) overnight at 4 °C. After washing with TBST three times, the membranes were incubated with an HRP-conjugated secondary antibody (Proteintech, China) at room temperature for 1 h. β-actin/GAPDH (Proteintech, China) was used as the standard loading control. Membranes were visualized using the ECL chemiluminescence detection kit (Yeasen Biotechnology, China).The antibodies applied in this study are as following: *FERMT2* (Proteintech, 11453-1-AP); *α-SMA* (Abcam, ab5694); Fibronectin (Proteintech, 60239-1-Ig); *GAPDH* (Proteintech, 60004-1-Ig)

2.7. Multiplex immunochemistry (mIHC) staining of human tissues in pan-cancer

Resected tumor tissues were initially fixed in 4 % paraformaldehyde before paraffin embedding. The resultant tissue sections (4 μm) underwent a 2-h baking step at 65 °C in an oven, followed by xylene dewaxing and gradual rehydration through a series of alcohol gradients. Afterwards, mIHC kits (AKOYA Biosciences, USA, NEL820001KT) were applied to stain the tissue sections aforementioned, adhering to the guidelines provided by the manufacturer. Tissue sample images were then captured using the Akoya Phenocycler Fusion system (AKOYA Biosciences, USA) and subsequently processed utilizing Phenochart software (version 1.2.0). The selected antibodies were employed as per recommended dilutions and incubation times, with details outlined in Table S1.

2.8. Potential in immunotherapy prediction and drug sensitivity analysis

Based on the Tumor Immune Dysfunction and Exclusion (TIDE) database, the "Biomarker Evaluation" unit,can perform the comparison between the expression level of *FERMT2* and other already published biomarkers using their predictive ability for response outcomes and prognosis. We utilized the "Drug sensitivity" module within the Gene Set Cancer Analysis (GSCA) online database to investigate the association between *FERMT2* expression levels and diverse tumor drug resistance patterns. Leveraging relevant drug data from the GDSC and CTRP databases, we identified the top 10 drugs that exhibited the strongest positive and negative correlations with *FERMT2* expression.

2.9. Cell lines

The immortalized cancer-associated fibroblasts after transformation were separated from human gastric cancer tissues, generously provided by my friend, Dr. Che Gang (The First Affiliated Hospital of Zhejiang University). CAFs were cultured in the Dulbecco's modified Eagle's medium (DMEM, Gibco, USA),supplemented with 10 % FBS, and kept in a 37 °C incubator with a 5 % CO2 humidified atmosphere.

2.10. RNA interference

The small interfering RNA targeting *FERMT2 as well as the* corresponding negative control was designed by Qingke Biotech (Guangzhou, China).Three sequences targeting *FERMT2* (sense 5′–3′) *are as follows:* si-1: CCUUGCUGCUCCGAUUCAA (dT) (dT); si-2: GCCCAGGACUGUAUAGUAA (dT) (dT); si-3: GCUAGAUGACCAGUCUGAA (dT) (dT). And the negative control sequence is 'UUCUCCGAACGUGUCACG UTT'. CAFs cultured in 6-well plates were transfected with si-RNA according to the manufacturer's instructions when reaching 60–80 % confluence. And the knockdown efficiency was confirmed using the western-blot method.

2.11. Statistical analysis

All bioinformatics analyses were conducted applying R software (4.2.1). Based on the distribution and variances of the data, either the Student's t-test or the Wilcoxon test was applied for analyzing continuous variables. One-way ANOVA analysis was used for comparison of continuous variable differences among multiple groups. The two-sided log-rank test was utilized to compare survival curves. All p-values were two-tailed, and the statistical significance threshold was defined as $P < 0.05$.

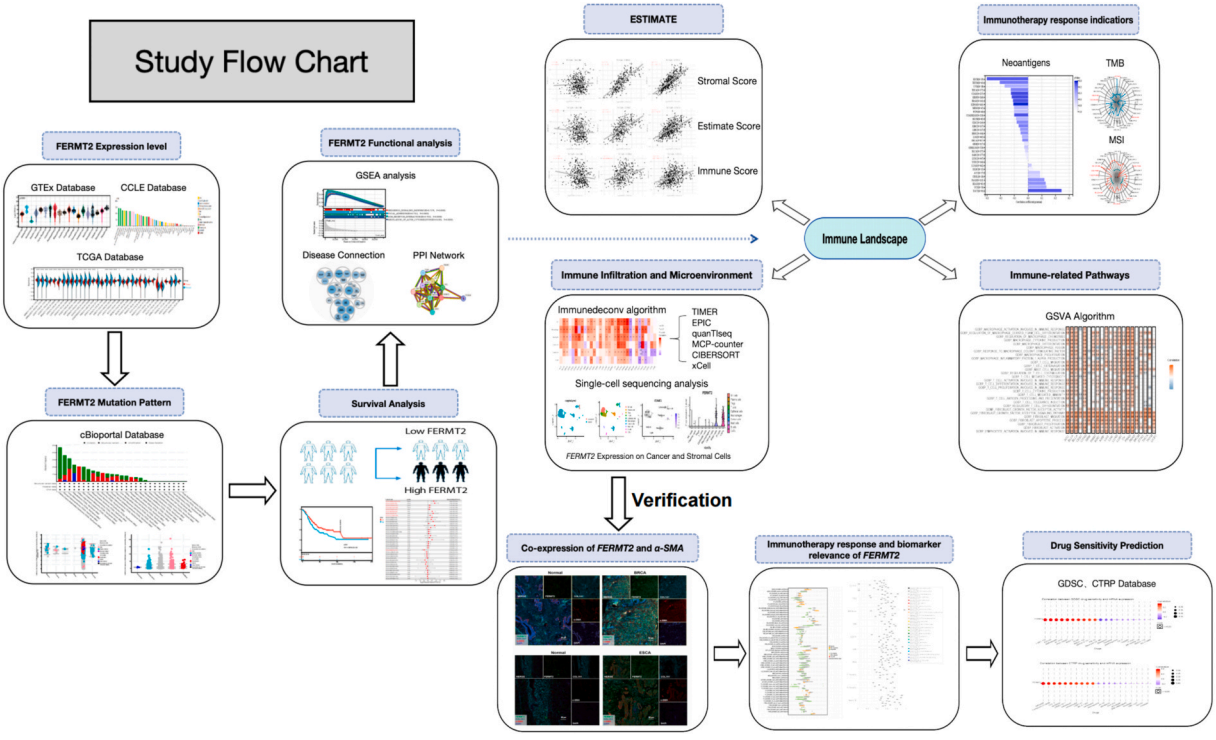

Fig. 1. The flow chart depicting the entire study process.

3. Results

3.1. Expression and genetic alterations of FERMT2

This study, based on the TCGA database, incorporated samples of various cancer types for comprehensive Investigation. The design

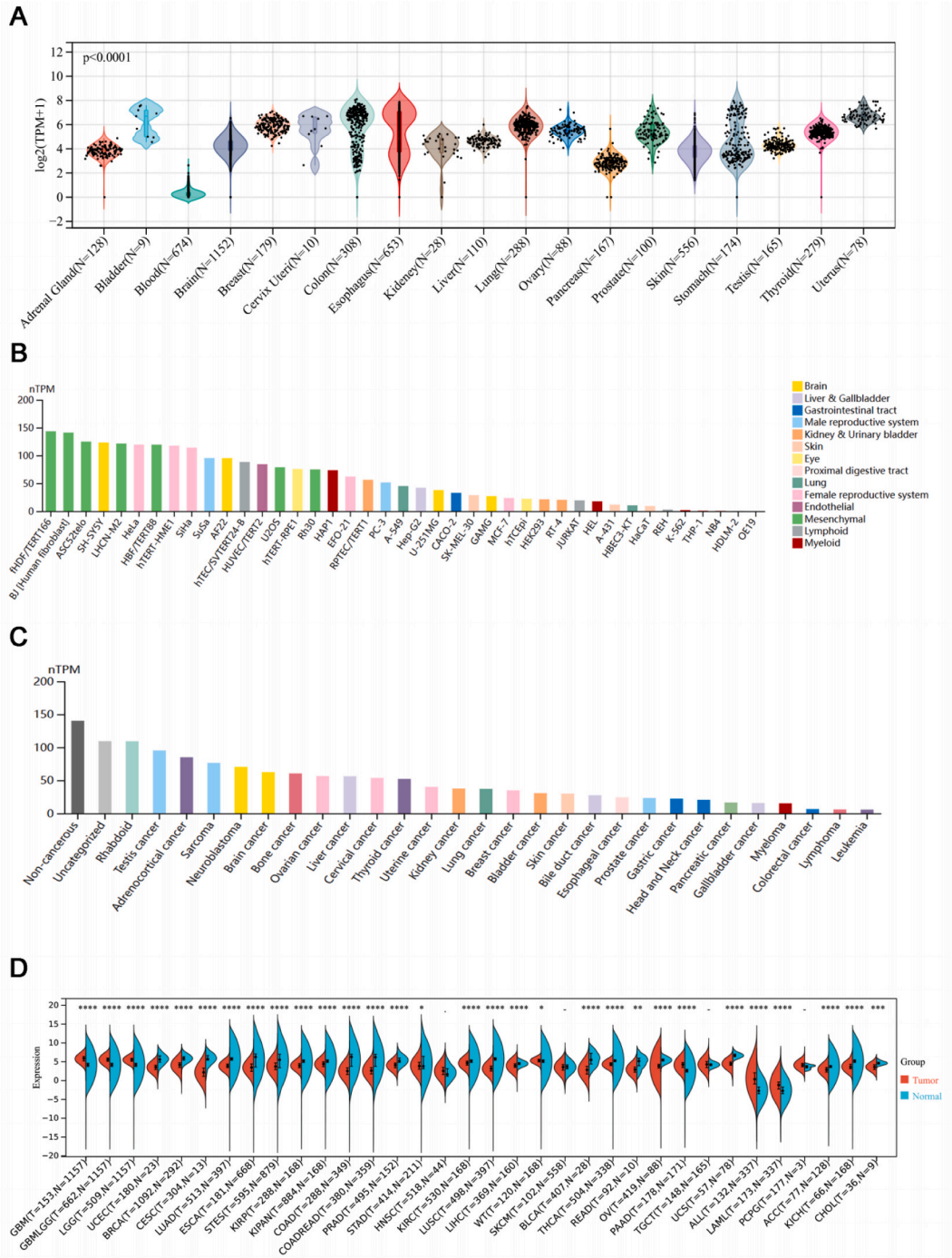

Fig. 2. Expression profile of *FERMT2*. *FERMT2* expression in non-cancerous human tissues sourced from the GETx dataset (A). *FERMT2* expression in cancer cell lines obtained from the CCLE dataset (B). *FERMT2* expression in tumor cell lines sourced from the HPA dataset (C). Comparison of *FERMT2* expression [log2 (x+0.001)] using TCGA and GETx datasets (D). Significance levels denoted as: *p < 0.05, **p < 0.01, ***p < 0.001, -, not statistically significant.

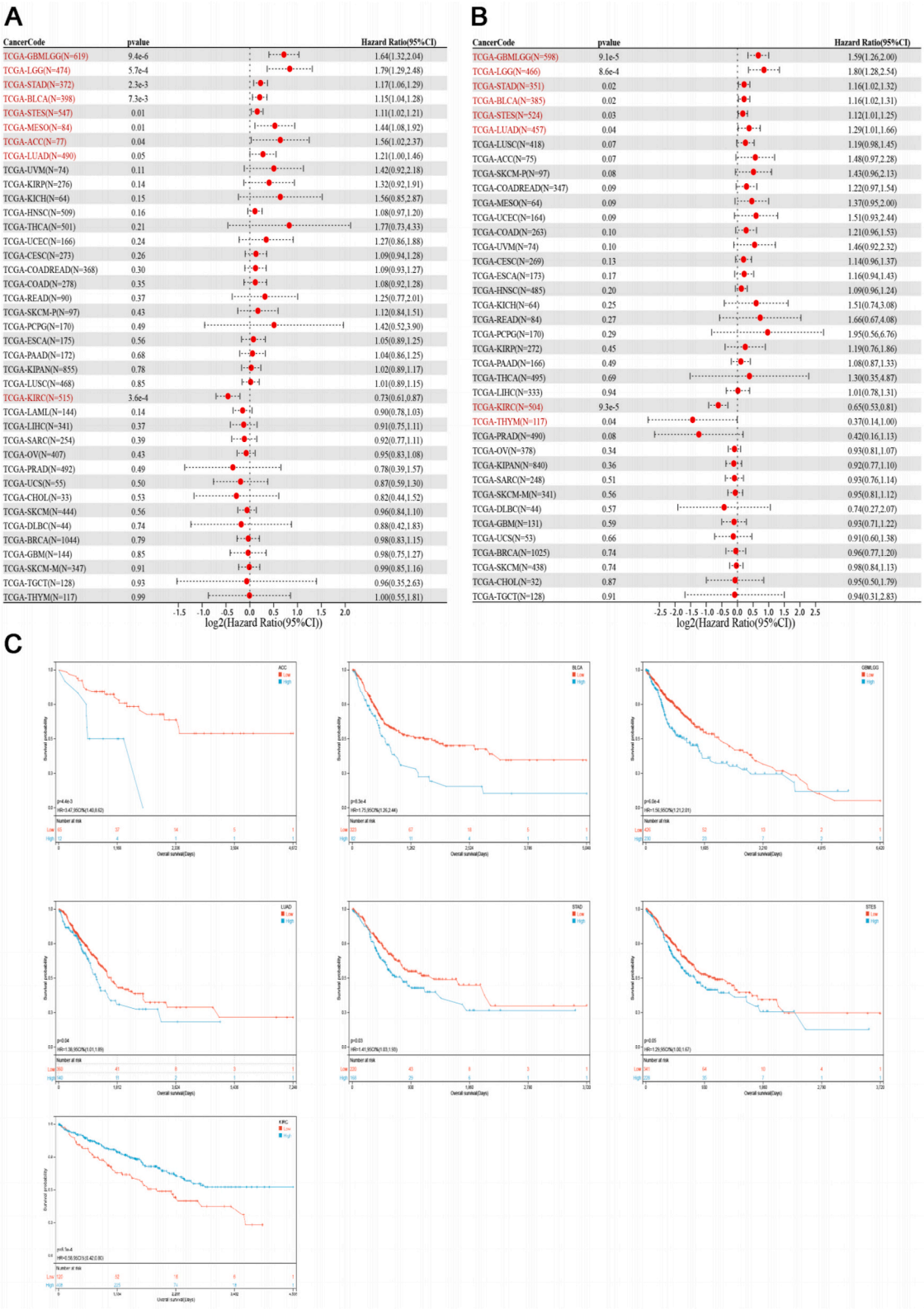

Fig. 3. Pan-cancer survival analysis of *FERMT2* using TCGA database. Survival analysis of *FERMT2* for OS (A) and DSS (B) in pan-cancer, illustrated through a forest plot. Prognostic impact of *FERMT2* on Overall Survival presented using the Kaplan-Meier method (C).

of this study is schematically illustrated in Fig. 1. Detailed identifiers of samples as well as datasets implemented in this study can be obtained in Supplementary file (Supplementary Table 1).

To comprehensively elucidate expression patterns of *FERMT2* across normal and cancerous samples, we scrutinized the expression

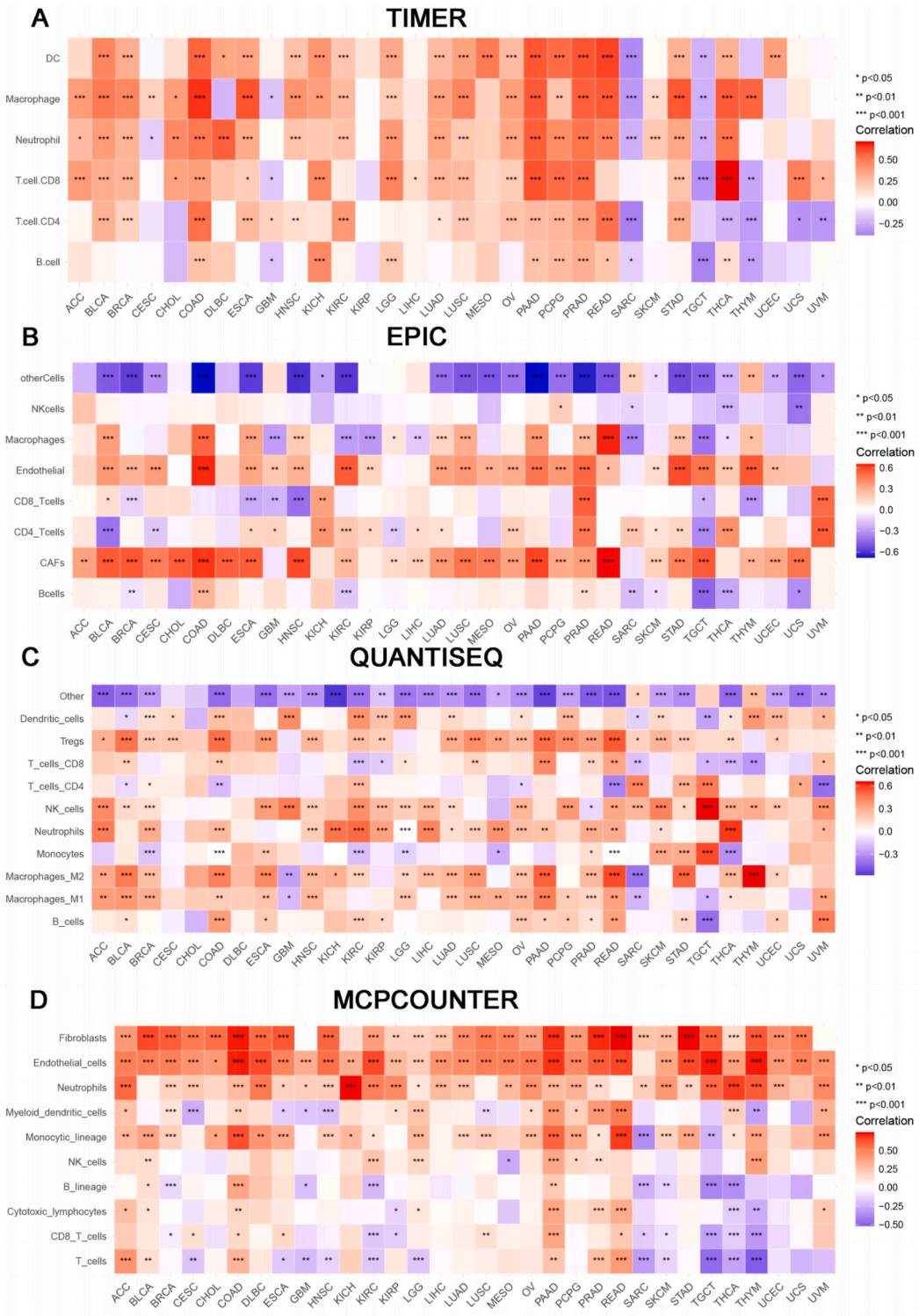

Fig. 4. Association between *FERMT2* expression levels and immune infiltration within TME. Analysis conducted through various algorithms including TIMER (A), EPIC (B), QUANTISEQ (C), and MCP-counter (D). Significance denoted as: *p < 0.05, **p < 0.01, ***p < 0.001.

level of *FERMT2* within a cohort of normal tissue samples from the GTEx dataset (Fig. 2A). This analysis revealed variable expression levels of *FERMT2* across these non-cancerous tissues. Notably, the colon, esophagus, uterus, stomach, and breast emerged as the top five tissues showcasing the highest enrichment of *FERMT2* expression. Data from the HPA dataset showed the TERT166, BJ (Human Fibroblast), ASC52telo, SH-SY5Y, and LHCN-M2 cell lines with the highest *FERMT2* RNA enrichment levels (Fig. 2B). Based on CCLE data, *FERMT2* exhibited prominent expression in tumor cell lines, particularly in rhabdoid, testis cancer, adrenocortical cancer, sarcoma, and neuroblastoma (Fig. 2C). Data of TCGA and GTEx dataset revealed a significant increase in *FERMT2* expression [log2 (x+0.001)] in cancer samples compared to normal controls across cancer types, including ALL, GBM, LAML, LGG, PAAD, PCPG, and STAD (Fig. 2D, $P < 0.05$).

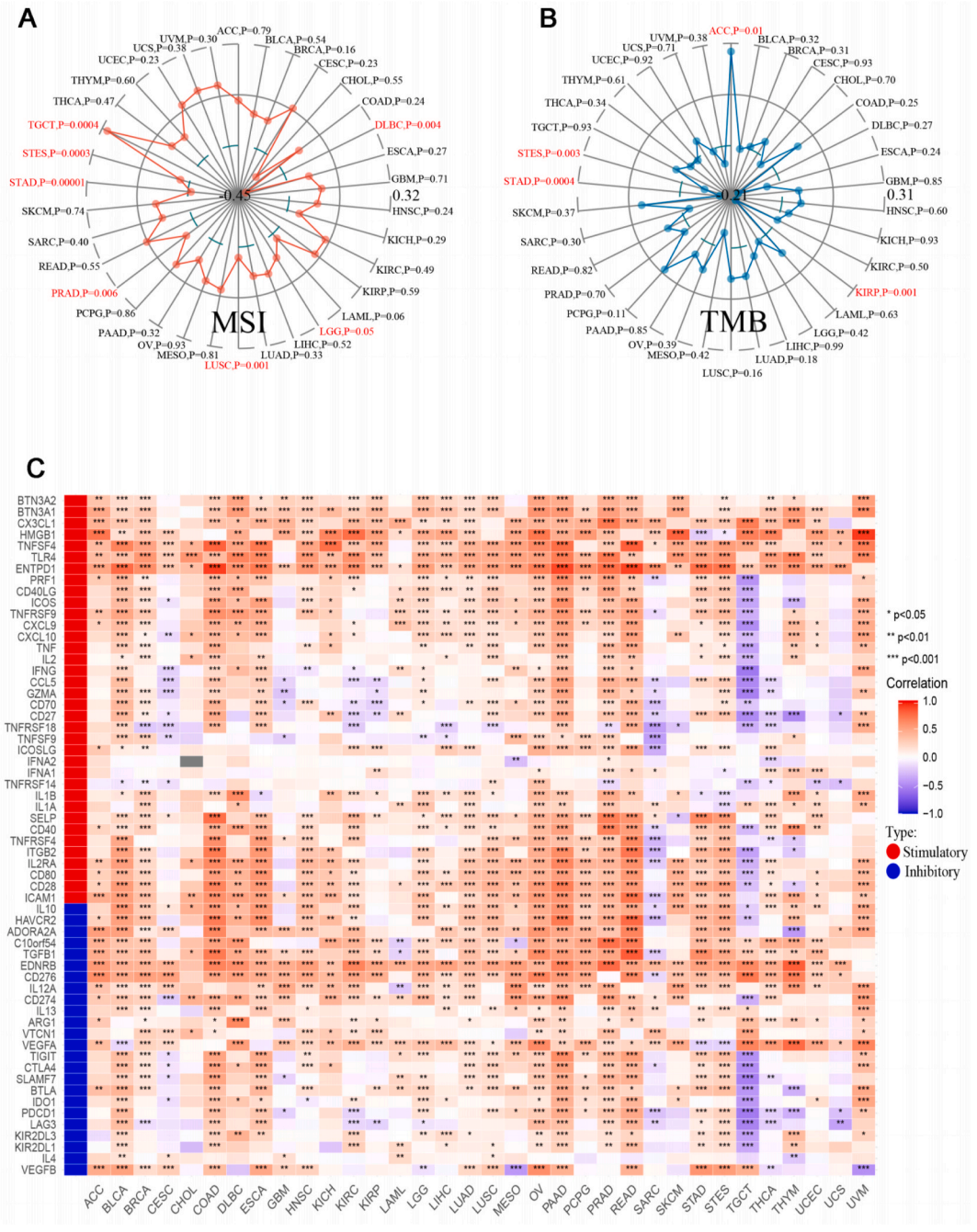

Fig. 5. Associations between *FERMT2* expression and key factors related with immunotherapy response (MSI, TMB, and immune checkpoint expression) in pan-cancer. Visualization of the relationship between *FERMT2* expression and MSI, TMB using a radar chart (A, B). Heatmap of the connection between *FERMT2* expression and immune checkpoint markers (C). Significance levels denoted as: *$p < 0.05$, **$p < 0.01$.

Furthermore, we analyzed the mutational landscape of *FERMT2* across diverse cancers based on the cBioPortal dataset (Fig. S1). Notably, UCEC, STAD, and LUAD stood out with significant mutation rates, exceeding an alteration frequency of 3 % (Figs. S1A and B). Simultaneously, we examined the interrelation between *FERMT2* mRNA expression patterns, mutational modes (Fig. S1C), and alterations of copy-number (Fig. S1D). Notably, our analysis revealed 88 mutations (68 missense, 14 truncating, 5 splice, and 1 fusion) within amino acids 100 to 600 (Fig. S1E).

3.2. *FERMT2* as a prognostic indicator

Subsequently, we proceeded to uncover the prognostic implications of *FERMT2* within various cancers types using Kaplan-Meier (KM) analysis. *FERMT2* demonstrated noteworthy prognostic significance in forecasting both overall survival (Fig. 3A) and disease-specific survival (Fig. 3B) across multiple tumor types. Increased *FERMT2* levels were notably linked to shorter overall survival in ACC, BLCA, GBM, LUAD, STAD, and STES, while conversely, in KIRC, elevating *FERMT2* expression was correlated with extended overall survival (Fig. 3C).

3.3. The Immunoregulatory role of FERMT2 in the TME

To unravel the immune-related implications of *FERMT2* within the tumor micro-environment across a spectrum of cancers, we applied the ESTIMATE algorithm to quantify the associations between *FERMT2* expression patterns and immune scores (Fig. S2), estimate scores (Fig. S3), as well as stromal scores (Fig. S4) in 35 distinct cancer types. Among these, notably, the three highest-ranking tumors exhibiting significant correlations between *FERMT2* expression levels and stromal scores were COAD, STAD, and BLCA. Similarly, substantial correlations between *FERMT2* and immune scores were found in COAD, READ, and TGCT, while for estimating scores, COAD, PAAD, and BLCA exhibited the most pronounced associations. Furthermore, we examined the association between

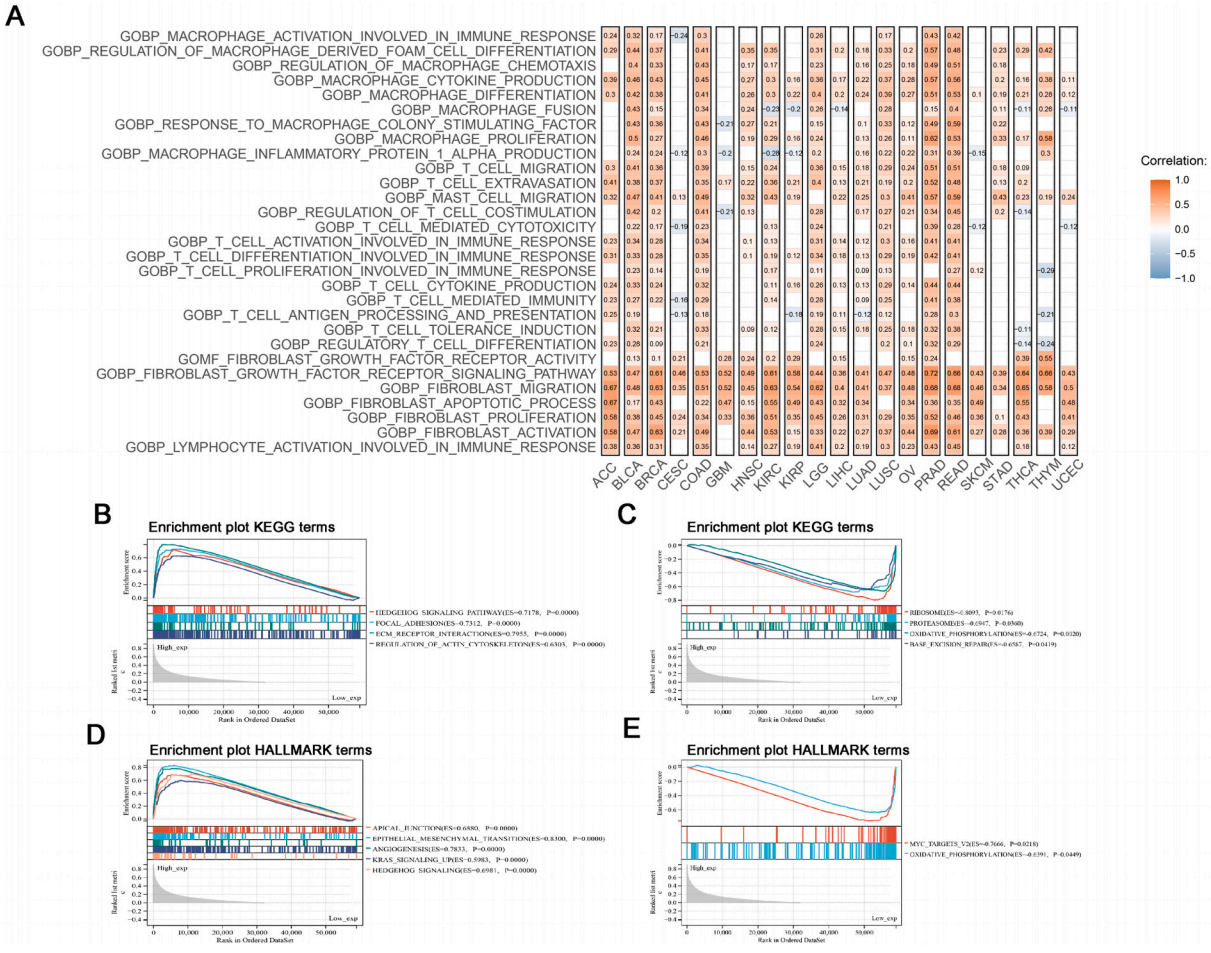

Fig. 6. Functional analysis of *FERMT2* in a pan-cancer context. Enrichment pathways of *FERMT2* identified using the GSVA algorithm (A). Top four positively enriched pathways (B) and top four negatively enriched pathways (C) based on KEGG terms. Top five positively enriched pathways (D) and top two negative enriched pathways (E) based on HALLMARK terms.

FERMT2 and neoantigens across human cancers (Fig. S5). The association between *FERMT2* expression patterns and the abundance of neoantigens in KIPAN, TGCT, and COAD ($p < 0.05$) was uncovered in this study.

Taking a step further, we aimed to elucidate the intricate interplay between *FERMT2* and immune cell populations within TME across a spectrum of cancers. we conducted a comprehensive analysis involving the application of six distinct algorithms for immune cell quantification (Fig. 4A–D, Figs. S6A–B).

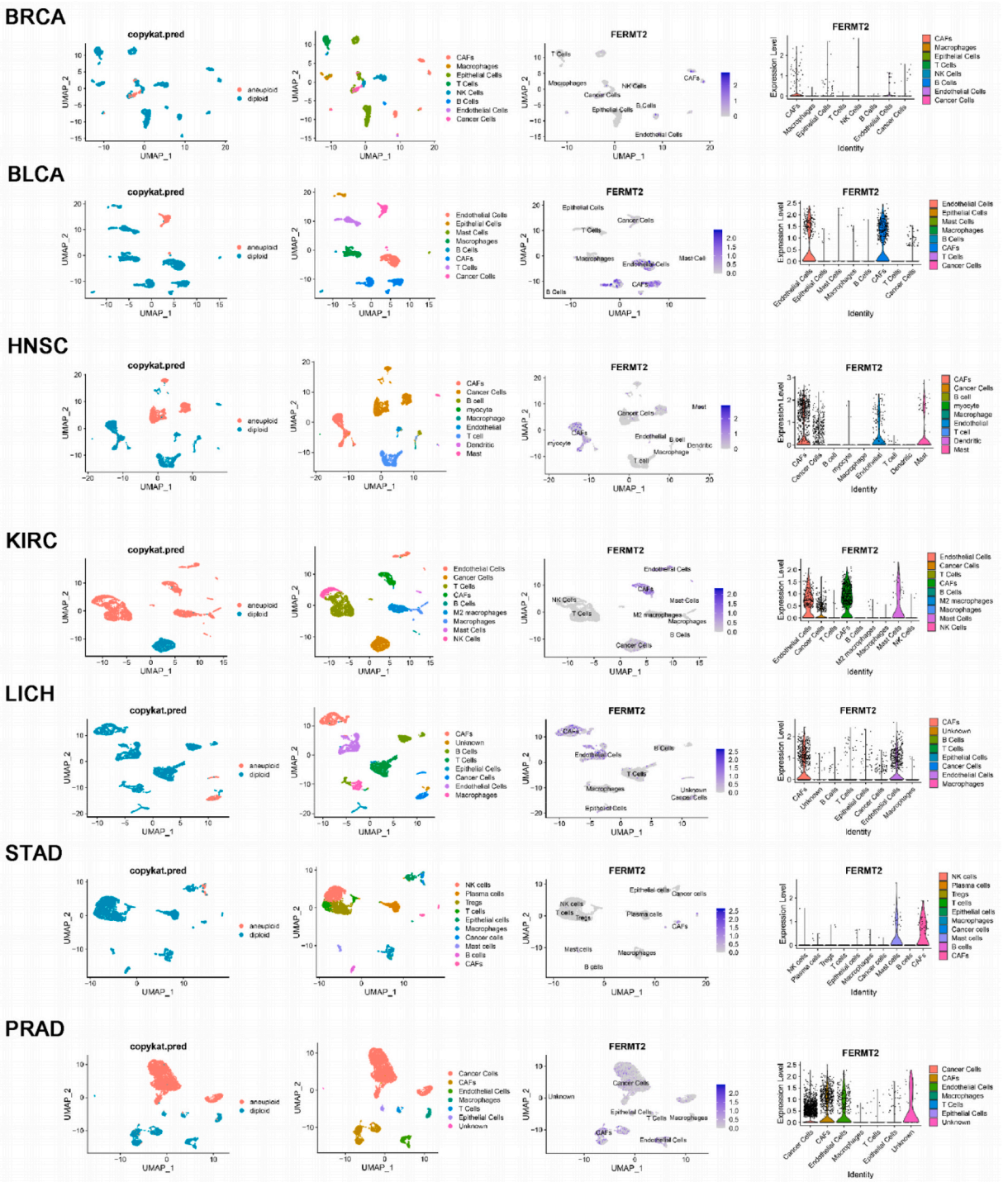

Fig. 7. Co-expression of *FERMT2* in both tumor and stromal cells in pan-cancer context based on SC-sequencing data. Examination of *FERMT2* expression levels within tumor and stromal cells in BRCA (A), BLCA (B), HNSC (C), KIRC (D), LICH (E), STAD (F), PRAD (G).

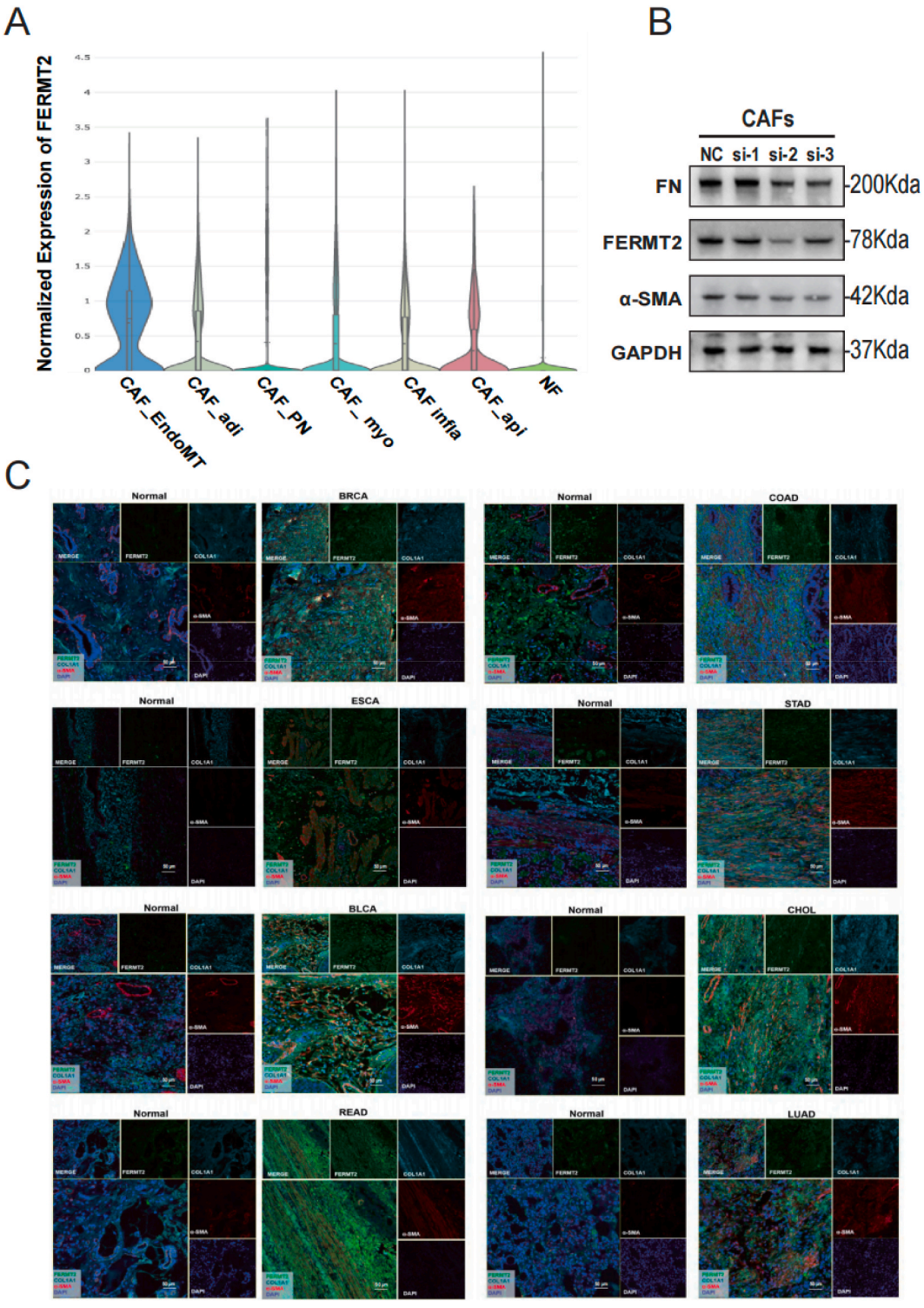

Fig. 8. A violin plot comparing the expression of *FERMT2* in the subtypes of CAFs and NFs in Luo et al.'s sc-RNA seq data set (A). The knockdown of *FERMT2* leads to a suppression of *α-SMA* and Fibronectin expression at the protein level in CAFs (B). Verification of *FERMT2* co-expression on cancer cells and CAFs in pan-cancer via multiplex immunofluorescence staining (C).The uncropped versions of Fig. B were provided as supplementary material.

Our findings unveiled the association between *FERMT2* expression levels and these immune-related cell populations within the comprehensive cohort. Particularly noteworthy was the significant positive correlation between elevated *FERMT2* expression and CAFs, endothelial cells, macrophages, and neutrophils across the majority of cancer types. Conversely, we observed a significant negative association between *FERMT2* and T cells along with B cells in specific cancers, including GBM, KIRC, SARC, SKCM, TGCT, THCA, and THYM (Fig. 4A, B, D, $P < 0.05$). Moreover, escalated *FERMT2* levels exhibited a significant association with both M1 and M2 macrophage subtypes in various cancer types (Fig. 4C, Fig. S6; $P < 0.05$). These findings collectively depicted the role of *FERMT2* in shaping the immune milieu across diverse cancers, shedding light on its potential as a pivotal player in the TME and its intricate crosstalk with various immune cell populations.

Furthermore, we observed distinct associations of *FERMT2* with MSI across various tumor types. Notably, in DLBC, LGG, LUSC, STES, STAD, and PRAD, *FERMT2* exhibited a negative correlation with MSI ($P < 0.05$). In contrast, we discovered a positive association between *FERMT2* and MSI was noted in TGCT (Fig. 5A, $P < 0.05$). In terms of TMB, our analysis revealed divergent relationships. Specifically, *FERMT2* exhibited a positive association with TMB in ACC ($P < 0.05$). To the contrast, it displayed a negative association with TMB in KIRP, STAD, and STES (Fig. 5B). Subsequently, we delved into the interrelation between *FERMT2* expression patterns and established immune-related checkpoints, encompassing *CX3CL1*, *CCL5*, *IFNA1*, *IL10*, *VEGFA*, *CTLA4*, and *C10orf54* (Fig. 5C). Notably, a substantial proportion of aforementioned pivotal molecules demonstrated a notably tight association with *FERMT2* expression patterns, particularly in BLCA, COAD, ESCA, KIPAN, OV, PAAD, PRAD, STES, and UVM.

In summary, our investigation underscores the pivotal role of *FERMT2* in modulating immune infiltrates across a pan-cancer context. Furthermore, it suggests that *FERMT2* holds the potential to emerge as a promising target of immunotherapy in the realm of tumor therapy.

3.4. Functional profiling based on FERMT2 expression Evaluation

Applying GSVA, based on GO terms, *FERMT2* displayed a notable positive association with immune-related pathways across diverse cancers, with particular prominence observed in BRCA, COAD, LGG, PRAD, and READ (Fig. 6A). Intriguingly, the majority of these pathways were correlated with fostering the fibroblasts activation and boosting, as well as pathways linked to macrophage activity.

Concurrently, we identified the foremost positively enriched pathways according to the KEGG terms, comprising HEDGEHOG SIGNALING_PATHWAY, FOCAL_ADHESION, ECM_RECEPTOR_INTERACTION, as well as REGULATION_OF_ACTIN_CYTOSKELETON (Fig. 6B; $P < 0.01$). Conversely, the leading negatively enriched pathways included RIBOSOME, PROTEASOME, OXIDATIVE_PHOSPHORYLATION, and BASE_EXCISION_REPAIR (Fig. 6C; $P < 0.05$). Regarding HALLMARK terms, the most significant positively enriched signal pathways encompassed APICAL_JUNCTION, EPITHELIAL_MESENCHYMAL_TRANSITION, and ANGIOGENESIS (Fig. 6D), however, the top two negatively enriched signal pathways including MYC_TARGET_V2 and OXIDATIVE_PHOSPHORYLATION (Fig. 6E; $P < 0.05$).

3.5. Unraveling FERMT2 expression in TME cell populations

Subsequently, we investigated the expression patterns of *FERMT2* on tumor as well as stromal cells within distinct cancer types, encompassing BRCA (Fig. 7 A), BLCA (Fig. 7 B), HNSC (Fig. 7 C), KIRC (Fig. 7 D), LICH (Fig. 7 E), STAD (Fig. 7 F), and PRAD (Fig. 7G). Remarkably, our study revealed the robust co-expression of *FERMT2* on malignant tumor epidemic cells as well as stromal cells in these specific cancers, particularly in CAFs. Utilizing the OPEN TARGET platform, we further illuminated the involvement of *FERMT2* in diverse diseases (Fig. S7A), along with insights into its protein-protein interactions (PPI) through network analysis (Fig. S7B).

3.6. Validation of co-expression of FERMT2 and α-smooth muscle actin (α-SMA)

The violin plot compares *FERMT2* expression levels across distinct fibroblast subtypes, encompassing both CAFs and NFs. The expression of *FERMT2* in normal fibroblast cells is markedly lower compared to that in CAFs (Fig. 8A). Additionally, the knockdown of *FERMT2* leads to a suppression expression of *α-SMA* and Fibronectin protein in CAFs (Fig. 8B). Furthermore, mIHC staining was utilized to validate the co-expression of *FERMT2* and *α-SMA* in tissues across various cancer types. *FERMT2* was fluorescently labeled in green (520), *COL1A1* in cyan (480), *α-SMA* in red (690), and DAPI was utilized for nuclear staining in blue. In comparison to the adjacent normal tissue, the tumor exhibits a significantly elevated presence of CAFs along with an increased expression of *FERMT2*. Noteworthy is the robust co-expression of *FERMT2* with *α-SMA* in CAFs within the tumor samples, observed consistently across various types of cancer (Fig. 8C, Fig. S8).

3.7. Prediction of immunotherapeutic Responsiveness and drug sensitivity associated with FERMT2 expression

Finally, to thoroughly explore the potential usefulness of FERMT2 as a novel immune target across various cancer types, we conducted predictive analyses encompassing immunotherapy response and drug sensitivity, both upon *FERMT2* expression levels (Fig. S9).

We evaluated the relevance of FERMT2 as a biomarker by comparing it with established biomarkers known for predicting immunotherapy response in human immunotherapy cohorts.Intriguingly, our analysis revealed that *FERMT2*, when evaluated independently, demonstrated an AUC surpassing 0.5 across seven out of the twenty-five immunotherapy cohorts (Fig. S9A). Remarkably,

this performance aligns with the predictive capabilities observed for T as well as B cell clonality, which similarly exhibited AUC values more than 0.5 across seven immunotherapy cohorts.

Meanwhile, it is noteworthy that *FERMT2* emerged as a robust predictor of immunotherapy response in the majority of murine immunotherapy cohorts. Responders consistently exhibited lower *FERMT2* expression levels, in contrast to non-responders who demonstrated the even or the elevated *FERMT2* expression (Fig. S9B).

Basing on the GDSC dataset, our analysis unveiled a correlation between *FERMT2* levels and drug sensitivity. Intriguingly, increased *FERMT2* expression was associated with reduced sensitivity to Bleomycin (inducer of DNA damage), Elesclomol (Selective antioxidant), and docetaxel (inhibitor of microtubule assembly), while concurrently enhancing the sensitivity to I-BET-762 (inhibitor for bromodomain and extra-C terminal domain proteins), WZ3105, Methotrexate (inhibitor for dihydrofolate reductase) (Fig. S9C). Meanwhile, in the CTRP database, increased *FERMT2* expression was associated with reduced sensitivity to staurosporine, JW-55, and abiraterone, while concurrently enhancing the sensitivity to belinostat, Compound 23 citrate, COL-3 (Fig. S9D).

These findings underscore the immunotherapeutic potential of *FERMT2* across diverse cancers. Furthermore, the prediction of a range of potential targeted drugs offers valuable insights, potentially guiding the development of *FERMT2*-targeted immunotherapies for pan-cancer treatment.

4. Discussion

Kindlins constitute an emerging family of focal adhesion proteins, with *Kindlin-2* being extensively studied. Kindlin-2, also referred to as FERMT2, is expressed in epithelial cells, striated cells, as well as smooth muscle cells. Notably, *FERMT2* engages with ILK and Migfilin, establishing a connection to the actin cytoskeleton and co-localizing with E-cadherin at cell-cell junctions [23].

Integrin affinity regulation is indispensable for both metazoan development and pathological processes. Meanwhile, the pivotal role of *FERMT2* in bidirectional integrin signaling is highlighted through its interactions with integrin β tails, as its loss disrupts integrin activation, resulting in lethality during peri-implantation due to detachment of the endoderm and epiblast from the basement membrane [24,25].

In the context of muscle development, *FERMT2* emerges as an integrin-associated factor, pivotal for myogenic differentiation via the activation of Wnt/β-catenin signal pathway [26]. And study has revealed the crucial role of *FERMT2* in skeletal development and chondrocyte differentiation regulation [27]. Furthermore, in recent studies, *FERMT2* was discovered to involve in the local and remote progression of numerous cancer types. *FERMT2* promotes breast cancer invasion and tumor formation by inducing hypermethylation-mediated downregulation of the miR-200 family [28]. *FERMT2* is correlated with aggressive clinicopathological features, and promotes invasion, metastasis as well as EMT of hepatocellular carcinoma cells via the activation of Wnt/β-catenin pathway [29]. In TME, *FERMT2* attributes to proliferation as well as metastasis of breast cancer by influencing host macrophages through *FERMT2/TGF-β/CSF-1* signaling axis [30]. Collectively, these insights underscore the intricate roles *FERMT2* play in integrin signaling and cancer-related biological processes, shedding light on their significance in diverse physiological and pathological contexts.

Cancer, a genomic disorder, is normally defined by genomic instability that results in point mutations together with structural changes, leading to presence of tumor antigens that trigger immune responses [31,32]. The immune system's involvement in immunosurveillance is vital [33], with adaptive and innate immune cells infiltrating TME to modulate tumor progression [34]. Various modalities of cancer immunotherapy, encompassing oncolytic viral interventions, cancer vaccination, cytokine-based treatments, adoptive cellular transfer, and inhibitors targeting immune checkpoints, have advanced and exhibited encouraging outcomes in clinical application.

Among these therapeutic strategies, ICIs have been transitioned into clinical practice and assumed a promising role in immunotherapeutic approaches. The fundamental purpose of ICIs is to rejuvenate the immune response against tumors through disruption of coinhibitory signaling pathways, thereby fostering immune-driven eradication of cancerous cells. Therapeutic targets predominantly employed for ICIs are *CTLA-4*, *PD-1*, and *PD-L1* [35,36]. TMB quantifies errors in somatic gene sequences, measured as the total anomalies (substitutions, insertions, deletions) per million bases. Elevated TMB levels may indicate enhanced potential for favorable outcomes in tumor immunotherapy [37]. MSI results from new microsatellite alleles in tumors compared to normal tissues, often due to repeat unit insertions or deletions. This is linked to deficient DNA mismatch repair in tumor cells. Notably, gastrointestinal tumors with MSI-High status generally respond favorably to treatment [38].

In our study, a comprehensive analysis was conducted into the role of *FERMT2* as an emerging immunotherapy target within TME across 33 different cancer types. Our investigation uncovered a substantial correlation between *FERMT2* and various immune-parameters, encompassing immune score, estimate score, and stromal score, across multiple cancer types. Furthermore, a significant association between *FERMT2* expression and pivotal indicators of immunogenicity, such as neoantigens, MSI, and TMB, was observed across this diverse set of cancers. Additionally, our research discovered a noteworthy positive association between *FERMT2* and several established immune checkpoint molecules, including *CD274, CD276, EDNRB, VEGFA, PDCD1, TGFB1*. These findings collectively emphasize the potential significance of *FERMT2* as an emerging immunotherapeutic target, capable of influencing various facets of the immune response within the TME.

Cancers are intricate systems consisting of malignantcells and a plethora of non-malignant cells, situated within a modified extracellular matrix (ECM). TME encompasses a variety of immune cell subtypes, CAFs, endothelial cells, pericytes, and other resident tissue cells [39]. Once deemed passive observers of tumorigenesis, these host cells are now recognized as pivotal contributors to the oncogenic processes underlying cancer development [40,41]. Furthermore, the plasticity of the tumor stroma could be taken advantage of through the reprogramming of cells in the TME as a potential strategy for cancer treatment [42].

Fibroblasts represent a widespread and heterogeneous cellular population within tissue of connection, which play a pivotal role in synthesizing ECM and basement membrane constituents, facilitating wound healing, influencing differentiation of neighboring epithelial cells and the development of tumors, orchestrating immune reactions, and maintaining homeostasis [43,44]. CAFs, consisting of fibroblasts and myofibroblasts, release higher levels of *SDF-1* compared to NFs. Meanwhile, CAFs originate from diverse sources, exhibiting significant heterogeneity, and can be identified using specific markers. Among these markers, fibroblast activation protein-alpha (*FAP*) and alpha-smooth muscle actin (*α-SMA*) are the most commonly used indicators for identifying CAFs [45]. Furthermore, CAFs helps to enhance tumor angiogenesis, and increase collagen contractility, attributing to boosting tumor progression [46]. Notably, the transformation of NFs into CAFs can be facilitated via autocrine *TGF-β* and *SDF-1* signaling [47]. In TME, CAFs gather and, stimulated by cellular factors encompassing *TGF-β*, *MCP1*, as well as *FGF* [44,48]. Once activated, CAFs become a primary supplier of secreted growth factors that facilitate tumorigenesis. This includes *VEGF*, acknowledged for its involvement in fostering vascular permeability and angiogenesis [49]. Additionally, CAFs initiate pro-inflammatory *NFκB* signaling, cultivating a pro-tumorigenic milieu evident in pre-neoplastic lesions [50].

As a summary, the expression patterns of *FERMT2* in tumor cells, as well as in stromal cells, were explored in pan-cancer context using single cell sequencing data. The expression level of *FERMT2* was elevated in cancer cells as well as stromal cells, especially CAFs and endothelial cells, in most cancers. Meanwhile, the knockdown of *FERMT2* leads to a suppression of *α-SMA* expression at the protein level in CAFs. Additionally, mIHC staining method was used to verify the co-expression of *FERMT2* with *α-SMA* within tumor samples across various cancer types. The aforementioned experimental results demonstrated that there was a significant correlation between *FERMT2* and activation of CAFs.

There's a growing trend in medical research involves employing public sequencing data and artificial intelligence models to identify personalized therapeutic methods [51]. Hence, we utilized public databases and computational models to evaluate the predictive ability of *FERMT2* in immunotherapy response. Our findings revealed that *FERMT2* exhibited predictive value across 7 out of the 25 cohorts applying immunotherapy, of which the AUC values exceeding 0.5. Remarkably, this performance aligns with the predictive capabilities observed for T together with B cell clonality, which similarly exhibited AUC values surpassing 0.5 across 7 immunotherapy cohorts. Furthermore, gene expression-based predictions identified potential therapeutic agents associated with *FERMT2* based on the CTRP database, providing a theoretical foundation for drug development targeting *FERMT2*.

5. Conclusions

In summary, our study illuminates the complex interplay among *FERMT2*, prognostic implications, and immune modulation across diverse cancer types, highlighting its potential as a viable candidate for innovative immunotherapeutic strategies. And we discovered the specific co-expression between *FERMT2* and *α-SMA* in CAFs across various cancer types. Consequently, therapies directed at *FERMT2* within TME hold promise for extending the survival of individuals diagnosed with cancer. Nevertheless, upcoming efforts demand a more comprehensive investigation to delve more profoundly into the functional and mechanistic aspects at the cellular stratum.

Ethical approval and informed consent

Approval of the research protocol: This study was approved by the Clinical Research Ethics Committee of the First Affiliated Hospital of Zhejiang University (Approval No:2023-0954).

Informed consent: All patients gave their informed consent.

Animal studies: None.

Funding

This research was funded by Jinhua science and technology research project 2021-4-166; And the Key Research and Development Program of Science and Technology Department of Zhejiang Province (No. 2018C03022), the National Key Research and Development Program of China (2019YFE0117500), National Natural Science Foundation of China (No. 82302886).

Data availability statement

The study-related public dataset numbers was listed in the supplementary table(S1).

CRediT authorship contribution statement

Guang-hao Wu: Conceptualization. **Chao He:** Writing – review & editing, Writing – original draft, Software. **Gang Che:** Software. **Zheng Zhou:** Software. **Bi-ying Chen:** Investigation. **Hai-ming Wu:** Investigation. **Jian-feng Chen:** Resources. **Wei-pu Zhu:** Funding acquisition. **Yan Yang:** Funding acquisition. **Zhan Zhou:** Methodology. **Li-song Teng:** Supervision. **Hai-yong Wang:** Writing – review & editing.

Declaration of competing interest

The authors declare that they have no known competing financial interests or personal relationships that could have appeared to influence the work reported in this paper.

Acknowledgments

We thanked all the R developers.

Appendix A. Supplementary data

Supplementary data to this article can be found online at https://doi.org/10.1016/j.heliyon.2024.e30505.

References

[1] F. Bray, M. Laversanne, E. Weiderpass, I. Soerjomataram, The ever-increasing importance of cancer as a leading cause of premature death worldwide, Cancer 127 (16) (2021 Aug 15) 3029–3030.
[2] J. Ferlay, M. Colombet, I. Soerjomataram, C. Mathers, D.M. Parkin, M. Piñeros, et al., Estimating the global cancer incidence and mortality in 2018: GLOBOCAN sources and methods, Int. J. Cancer 144 (8) (2019 Apr 15) 1941–1953.
[3] F. Bray, J. Ferlay, I. Soerjomataram, R.L. Siegel, L.A. Torre, A. Jemal, Global cancer statistics 2018: GLOBOCAN estimates of incidence and mortality worldwide for 36 cancers in 185 countries, Ca-cancer J Clin 68 (6) (2018 Nov) 394–424.
[4] H. Sung, J. Ferlay, R.L. Siegel, M. Laversanne, I. Soerjomataram, A. Jemal, et al., Global cancer statistics 2020: GLOBOCAN estimates of incidence and mortality worldwide for 36 cancers in 185 countries, CA Cancer J Clin 71 (3) (2021 May) 209–249.
[5] N.M. Anderson, M.C. Simon, The tumor microenvironment, Curr. Biol. 30 (16) (2020 Aug) R921–R925.
[6] Y. Xiao, D. Yu, Tumor microenvironment as a therapeutic target in cancer, Pharmacol. Therapeut. 221 (2021 May) 107753.
[7] M.Z. Jin, W.L. Jin, The updated landscape of tumor microenvironment and drug repurposing, Signal Transduct Tar 5 (1) (2020 Aug 25) 166.
[8] Y. Zhang, Z. Zhang, The history and advances in cancer immunotherapy: understanding the characteristics of tumor-infiltrating immune cells and their therapeutic implications, Cell. Mol. Immunol. 17 (8) (2020 Aug) 807–821.
[9] B. Li, H.L. Chan, P. Chen, Immune checkpoint inhibitors: Basics and challenges, Curr. Med. Chem. 26 (17) (2019 Aug 27) 3009–3025.
[10] A. Naimi, R.N. Mohammed, A. Raji, S. Chupradit, A.V. Yumashev, W. Suksatan, et al., Tumor immunotherapies by immune checkpoint inhibitors (ICIs); the pros and cons, Cell Commun. Signal. 20 (1) (2022 Apr 7) 44.
[11] K. Li, A. Zhang, X. Li, H. Zhang, L. Zhao, Advances in clinical immunotherapy for gastric cancer, Biochim. Biophys. Acta Rev. Canc 1876 (2) (2021 Dec) 188615.
[12] B. Burtness, K.J. Harrington, R. Greil, D. Soulières, M. Tahara, G. De Castro, et al., Pembrolizumab alone or with chemotherapy versus cetuximab with chemotherapy for recurrent or metastatic squamous cell carcinoma of the head and neck (KEYNOTE-048): a randomized, open-label, phase 3 study, Lancet 394 (10212) (2019 Nov) 1915–1928.
[13] R. Mukherji, D. Debnath, M.L. Hartley, M.S. Noel, The role of immunotherapy in pancreatic cancer, Curr. Oncol. 29 (10) (2022 Sep 23) 6864–6892.
[14] S. Tan, D. Li, X. Zhu, Cancer immunotherapy: pros, cons and beyond, Biomed. Pharmacother. 124 (2020 Apr) 109821.
[15] M. Yasuda-Yamahara, M. Rogg, J. Frimmel, P. Trachte, M. Helmstaedter, P. Schroder, et al., *FERMT2* links cortical actin structures, plasma membrane tension and focal adhesion function to stabilize podocyte morphology, Matrix Biol. 68–69 (2018 Aug) 263–279.
[16] W.C. Lin, L.H. Chen, Y.C. Hsieh, P.W. Yang, L.C. Lai, E.Y. Chuang, et al., miR-338-5p inhibits cell proliferation, colony formation, migration and cisplatin resistance in esophageal squamous cancer cells by targeting *FERMT2*, Carcinogenesis 40 (7) (2019 Jul 20) 883–892.
[17] K. Sossey-Alaoui, E. Pluskota, K. Bialkowska, D. Szpak, Y. Parker, C.D. Morrison, et al., *FERMT2* regulates the growth of breast cancer tumors by activating CSF-1-Mediated macrophage infiltration, Cancer Res. 77 (18) (2017 Sep 15) 5129–5141.
[18] N. Yoshida, A. Masamune, S. Hamada, K. Kikuta, T. Takikawa, F. Motoi, et al., *FERMT2* in pancreatic stellate cells promotes the progression of pancreatic cancer, Cancer Lett. 390 (2017 Apr 1) 103–114.
[19] X. Ma, D. Zhao, S. Liu, J. Zuo, W. Wang, F. Wang, et al., *FERMT2* upregulation in CAFS enhances EMT of OSCC and M2 macrophage polarization, Oral Dis. (2023 Jun 25; odi) 14610.
[20] X. Lu, C. Zhou, R.F. Li, J.W. Ye, W.L. Zhai, [*FERMT2* promotes gallbladder cancer metastasis and invasion by inducing epithelial-mesenchymal transition], Zhonghua Wai Ke Za Zhi 56 (8) (2018 Aug 1) 617–622.
[21] W. Xia, Z. Gao, X. Jiang, L. Jiang, Y. Qin, D. Zhang, et al., Alzheimer's risk factor *FERMT2* promotes the progression of colorectal carcinoma via Wnt/β-catenin signaling pathway and contributes to the negative correlation between Alzheimer and cancer, PLoS One 17 (12) (2022) e0278774.
[22] G. Sturm, F. Finotello, M. List, Immunedeconv: an R package for unified access to computational methods for estimating immune cell fractions from bulk RNA-sequencing data, Methods Mol. Biol. 2120 (2020) 223–232.
[23] S. Ussar, H.V. Wang, S. Linder, R. Fässler, M. Moser, The Kindlins: subcellular localization and expression during murine development, Exp. Cell Res. 312 (16) (2006 Oct 1) 3142–3151.
[24] E. Montanez, S. Ussar, M. Schifferer, M. Bösl, R. Zent, M. Moser, et al., *FERMT2* controls bidirectional signaling of integrins, Gene Dev. 22 (10) (2008 May 15) 1325–1330.
[25] D.S. Harburger, M. Bouaouina, D.A. Calderwood, Kindlin-1 and -2 directly bind the C-terminal region of beta integrin cytoplasmic tails and exert integrin-specific activation effects, J. Biol. Chem. 284 (17) (2009 Apr 24) 11485–11497.
[26] Y. Yu, L. Qi, J. Wu, Y. Wang, W. Fang, H. Zhang, Kindlin 2 regulates myogenic related factor myogenin via a canonical Wnt signaling in myogenic differentiation, PLoS One 8 (5) (2013) e63490.
[27] C. Wu, H. Jiao, Y. Lai, W. Zheng, K. Chen, H. Qu, et al., *FERMT2* controls TGF-β signalling and Sox 9 expression to regulate chondrogenesis, Nat. Commun. 6 (2015 Jul 7) 7531.
[28] Y. Yu, J. Wu, L. Guan, L. Qi, Y. Tang, B. Ma, et al., Kindlin 2 promotes breast cancer invasion via epigenetic silencing of the microRNA200 gene family, Int. J. Cancer 133 (6) (2013 Sep 15) 1368–1379.
[29] J. Lin, W. Lin, Y. Ye, L. Wang, X. Chen, S. Zang, et al., *FERMT2* promotes hepatocellular carcinoma invasion and metastasis by increasing Wnt/β-catenin signaling, J. Exp. Clin. Cancer Res. 36 (1) (2017 Sep 29) 134.
[30] K. Sossey-Alaoui, E. Pluskota, K. Bialkowska, D. Szpak, Y. Parker, C.D. Morrison, et al., *FERMT2* regulates the growth of breast cancer tumors by activating CSF-1–Mediated macrophage infiltration, Cancer Res. 77 (18) (2017 Sep 15) 5129–5141.
[31] M.R. Stratton, P.J. Campbell, P.A. Futreal, The cancer genome, Nature 458 (7239) (2009 Apr 9) 719–724.
[32] R.D. Schreiber, L.J. Old, M.J. Smyth, Cancer immunoediting: integrating immunity's roles in cancer suppression and promotion, Science 331 (6024) (2011 Mar 25) 1565–1570.

[33] M.D. Vesely, M.H. Kershaw, R.D. Schreiber, M.J. Smyth, Natural innate and adaptive immunity to cancer, Annu. Rev. Immunol. 29 (2011) 235–271.
[34] R.J. Seager, C. Hajal, F. Spill, R.D. Kamm, M.H. Zaman, Dynamic interplay between tumour, stroma and immune system can drive or prevent tumour progression, Converg Sci Phys Oncol 3 (2017) 034002.
[35] P. Sharma, J.P. Allison, The future of immune checkpoint therapy, Science 348 (6230) (2015 Apr 3) 56–61.
[36] Immune checkpoint targeting in cancer therapy: toward combination strategies with curative potential - PubMed [Internet]. [cited 2023 Aug 14]. Available from: https://pubmed.ncbi.nlm.nih.gov/25860605/.
[37] M. Yarchoan, A. Hopkins, E.M. Jaffee, Tumor mutational burden and response rate to PD-1 inhibition, N. Engl. J. Med. 377 (25) (2017 Dec 21) 2500–2501.
[38] A. Lin, J. Zhang, P. Luo, Crosstalk between the MSI status and tumor microenvironment in colorectal cancer, Front. Immunol. 11 (2020) 2039.
[39] K.E. de Visser, J.A. Joyce, The evolving tumor microenvironment: from cancer initiation to metastatic outgrowth, Cancer Cell 41 (3) (2023 Mar 13) 374–403.
[40] K.G.K. Deepak, R. Vempati, G.P. Nagaraju, V.R. Dasari, N. S, D.N. Rao, et al., Tumor microenvironment: challenges and opportunities in targeting metastasis of triple negative breast cancer, Pharmacol. Res. 153 (2020 Mar) 104683.
[41] Y. Jiang, C. Wang, S. Zhou, Targeting tumor microenvironment in ovarian cancer: premise and promise, Biochim. Biophys. Acta Rev. Canc 1873 (2) (2020 Apr) 188361.
[42] S. Ma, B. Sun, S. Duan, J. Han, T. Barr, J. Zhang, et al., YTHDF2 orchestrates tumor-associated macrophage reprogramming and controls antitumor immunity through CD8+ T cells, Nat. Immunol. 24 (2) (2023 Feb) 255–266.
[43] J.J. Tomasek, G. Gabbiani, B. Hinz, C. Chaponnier, R.A. Brown, Myofibroblasts and mechano-regulation of connective tissue remodelling, Nat. Rev. Mol. Cell Biol. 3 (5) (2002 May) 349–363.
[44] R. Kalluri, M. Zeisberg, Fibroblasts in cancer, Nat. Rev. Cancer 6 (5) (2006 May) 392–401.
[45] H. Li, E.T. Courtois, D. Sengupta, Y. Tan, K.H. Chen, J.J.L. Goh, et al., Reference component analysis of single-cell transcriptomes elucidates cellular heterogeneity in human colorectal tumors, Nat. Genet. 49 (5) (2017 May) 708–718.
[46] A. Orimo, R.A. Weinberg, Stromal fibroblasts in cancer: a novel tumor-promoting cell type, Cell Cycle 5 (15) (2006 Aug) 1597–1601.
[47] Y. Kojima, A. Acar, E.N. Eaton, K.T. Mellody, C. Scheel, I. Ben-Porath, et al., Autocrine TGF-beta and stromal cell-derived factor-1 (SDF-1) signaling drives the evolution of tumor-promoting mammary stromal myofibroblasts, P Natl Acad Sci Usa 107 (46) (2010 Nov 16) 20009–20014.
[48] T. Marsh, K. Pietras, S.S. McAllister, Fibroblasts as architects of cancer pathogenesis, Biochim. Biophys. Acta 1832 (7) (2013 Jul) 1070–1078.
[49] D. Fukumura, R. Xavier, T. Sugiura, Y. Chen, E.C. Park, N. Lu, et al., Tumor induction of VEGF promoter activity in stromal cells, Cell 94 (6) (1998 Sep 18) 715–725.
[50] N. Erez, M. Truitt, P. Olson, S.T. Arron, D. Hanahan, Cancer-associated fibroblasts are activated in incipient neoplasia to orchestrate tumor-promoting inflammation in an NF-kappaB-Dependent manner, Cancer Cell 17 (2) (2010 Feb 17) 135–147.
[51] N.R. Rydzewski, E. Peterson, J.M. Lang, M. Yu, S. Laura Chang, M. Sjöström, et al., Predicting cancer drug TARGETS - TreAtment response generalized elastic-neT signatures, NPJ Genom Med 6 (1) (2021 Sep 21) 76.